



**AUSTRALIAN ATOMIC ENERGY COMMISSION  
RESEARCH ESTABLISHMENT  
LUCAS HEIGHTS**

**MEASUREMENT OF THERMAL NEUTRON WAVES AT HIGH  
FREQUENCIES IN BeO**

by

**A.I.M. RITCHIE  
S. WHITTLESTONE**

**March 1972**

ISBN 0 642 99453 6



AUSTRALIAN ATOMIC ENERGY COMMISSION  
RESEARCH ESTABLISHMENT  
LUCAS HEIGHTS

MEASUREMENT OF THERMAL NEUTRON WAVES  
AT HIGH FREQUENCIES IN BeO

by

A.I.M. RITCHIE

S. WHITTLESTONE

ABSTRACT

The amplitudes and phases of neutron waves have been measured in a BeO assembly in the frequency range 515.7 Hz to 1719 Hz. The results confirm earlier measurements that below  $\sim 520$  Hz the neutron wave has the properties of a discrete mode of propagation. At frequencies  $\geq 720$  Hz the attenuation  $\alpha(z)$  and phase shift parameters  $\xi(z)$  change with distance from the source, the change being more marked the higher the frequency.

The observed spatial variations of  $\alpha(z)$  and  $\xi(z)$  do not agree with present theoretical predictions. Interference effects predicted by theory have not been observed.

National Library of Australia card number and ISBN 0 642 99453 6

The following descriptors have been selected from the INIS Thesaurus to describe the subject content of this report for information retrieval purposes. For further details please refer to IAEA-INIS-12 (INIS: Manual for Indexing) and IAEA-INIS-13 (INIS: Thesaurus) published in Vienna by the International Atomic Energy Agency.

AMPLITUDES; ATTENUATION; BERYLLIUM MODERATORS; BERYLLIUM OXIDES; DISPERSION RELATIONS; INTERFERENCE; NEUTRON DENSITY; NEUTRON TRANSPORT THEORY; PHASE SHIFT; SPATIAL DISTRIBUTION; THERMAL NEUTRONS; WAVE PROPAGATION

## CONTENTS

	<u>Page</u>
1. INTRODUCTION	1
2. EXPERIMENTAL METHOD	2
3. ERRORS	3
4. RESULTS AND DISCUSSION	6
5. CONCLUSIONS	9
6. REFERENCES	10

### APPENDIX A

### APPENDIX B

TABLE 1	Compilation of Amplitudes and Phases from Neutron Wave Experiments in BeO, at Frequencies 515.7, 736.6, 982.3, 1473.3 and 1719.0 Hz, Normalised to a density of $2.96 \text{ g cm}^{-3}$
TABLE 2	Effect of Source Conditions on 982.3 Hz Neutron Wave
FIGURE 1	Neutron Wave Amplitudes for BeO of Density $2.96 \text{ g cm}^{-3}$
FIGURE 2	Neutron Wave Phases for BeO of Density $2.96 \text{ g cm}^{-3}$
FIGURE 3	Neutron Wave Attenuation Parameters Derived from Fits to Data Between Z and Z + 10 cm From the Source, $Z \geq 7.35 \text{ cm}$
FIGURE 4	Neutron Wave Phase Shift Parameters Derived from Fits to Data Between Z and Z + 10 cm from the Source, $Z \geq 7.35 \text{ cm}$
FIGURE 5	Comparison Between Theoretical and Experimental $\alpha(z)$ and $\xi(z)$
FIGURE 6	Comparison of Experimental and Theoretical Amplitudes
FIGURE 7	Comparison of Experimental and Theoretical Phases
FIGURE 8	Dispersion Relations for Neutrons in BeO for an Assembly with $B^2 = 0.00513 \text{ cm}^{-2}$



## 1. INTRODUCTION

In a previous paper (Ritchie and Whittlestone 1971) the results of a neutron wave experiment in BeO in the frequency range 0-500 Hz were reported. The results indicated that from 9 cm to 42 cm from the source in a block 60.96 cm long the neutron wave had the properties of a discrete mode of propagation in the sense that the attenuation and phase shift constants did not change with distance. This was at variance with the rather simple minded approach that, since in BeO the sub-Bragg continuum (Duderstadt 1968, Williams 1968) is less attenuated with distance than the discrete mode it will dominate at large distances from the source and the wave properties will, in general, change with distance from the source. However, the attenuation constant  $\alpha$  and the phase shift constant  $\xi$  of this apparently discrete mode of propagation, were not in good agreement with the calculations of  $\alpha$  and  $\xi$  for the discrete mode (Wood 1969) and more importantly the thermal neutron diffusion parameters derived from the dispersion relations were not, in general, in agreement with the diffusion parameters derived from a pulsed experiment in the same block of material (Ritchie 1968). In particular, the diffusion coefficient from the wave experiment was  $\sim 9$  per cent higher than that from the pulsed experiment and could represent some contamination from the sub-Bragg continuum mode.

Wood (1971) has also reported some calculations of the effective propagation constant  $\rho(z, \omega)$  for BeO as seen by a  $1/v$  detector when the source has a Maxwellian distribution of energies. He shows that  $\alpha(z)$  and  $\xi(z)$  do in fact vary with distance, the variation increasing with increasing frequency. For example, at  $\omega = 2048$  rad/sec ( $f = 325.9$  Hz)  $\xi(z)$  changes by  $\sim 8$  per cent and  $\alpha(z)$  by  $\sim 6$  per cent over the range 10 to 40 cm from the source. Such a large change is not really consistent with the experimental results which showed that in this frequency range the parameters  $\alpha$  and  $\xi$  evaluated from sets of points 9 to 21 cm and 21 to 42 cm from the source agreed within the experimental errors of  $\sim 1$  per cent. It is clearly of interest to measure  $\alpha(z)$  and  $\xi(z)$  with greater precision to verify this apparent discrepancy between theory and experiment and find the frequency above which the experimental results do show  $\alpha(z)$  and  $\xi(z)$  to vary with distance.

Interference effects have been noted in wave experiments in graphite at frequencies in excess of  $\sim 350$  Hz (Utsuro et al. 1968, Takahashi and Sumita 1968a) and have been attributed to the interference between a

sub-Bragg and a thermal wave. Such interference effects have been reproduced theoretically using both simple two group theory (Utsuro and Shibata 1967, Takahashi and Sumita 1968b) and diffusion theory with a one term degenerate kernel (Nishina and Akcasu 1970). Interference effects in BeO have also been predicted by Wood and Lawrence (1971) and should appear in the range  $489 \leq f \leq 1400$  Hz and  $25 \leq z \leq 55$  cms. in an assembly of transverse buckling  $0.0048 \text{ cm}^{-2}$  which is very close to that of the BeO assembly previously investigated.

This paper reports some neutron wave experiments in BeO in the frequency range  $515.7 \text{ Hz} \leq f \leq 1719 \text{ Hz}$ . The experiments were designed primarily to note those frequencies at which the wave propagation was no longer compatible with a discrete mode of propagation but were also such that any pronounced interference effects should be measurable.

## 2. EXPERIMENTAL METHOD

The equipment used was essentially the same as that described in Ritchie and Whittlestone (1971). However, rather than use the sinusoidally modulated source described previously, the square wave modulation system installed on the 3 MeV Van de Graaff accelerator (Fraser et al. 1968) was used to produce square pulses with uniform mark space ratio. Apart from simplifying operation of the experiment, this increased the ratio of the fundamental frequency component to the average neutron density by a factor of  $\sqrt{2}$ , and permitted maximum utilisation of the beam current available from the accelerator. The fundamental frequency component was extracted by harmonic analysis of the measured time distributions.

As in the previous experiments, a cadmium shutter could be inserted between the BeO stack and the modulated neutron source. The wave measured with the shutter in place (the epi-cadmium wave) was subtracted from the wave measured with the shutter out (the total wave) to obtain the wave whose component neutrons had energies less than the cadmium cutoff (the sub-cadmium wave). The spatial distributions were again normalised using a fixed cadmium covered detector buried in the polythene moderator. However, rather than carrying out a measurement at a given point for a fixed monitor count, the duration of the run at each point was determined by the integrated count from the movable detector. This technique allowed reasonably good statistical accuracy to be achieved when the movable detector was far from the source and avoided excessive data accumulation at points close to the source. Typical values chosen



for this integrated count were  $2.7 \times 10^6$  when the shutter was out and  $9 \times 10^5$  when the shutter was in place.

Experiments were carried out at five different frequencies - 500.0, 714.2, 952.4 (three measurements), 1428.5 and 1666.7 Hz. The  $\text{Li}^7(\text{p},\text{n})\text{Be}^7$  reaction was used as the neutron source throughout (incident proton energy 2.0 MeV and thick lithium target). The polythene moderator was two inches thick in all cases except for one of the runs at 952.4 Hz where it was increased to three inches. The detector was again a 20th Century 1/4 inch diameter  $\text{BF}_3$  detector mounted with its long axis parallel to the incident beam direction (z-axis).

### 3. ERRORS

Errors in the neutron detection system, and the derivation of statistical errors in amplitudes and phases from the time distributions have been discussed in detail previously (Ritchie and Whittlestone 1971)

Because measurements at a given frequency took between 48 and 72 hours, long term changes in the neutron production system were more important than in the previous measurements. The chief factors were:-

- (i) Variation of beam energy
- (ii) Target deterioration
- (iii) Deuterium contamination of the proton beam

The accelerator potential was stabilised using the generating voltmeter as described by Whittlestone (1968). Operating with up to 250  $\mu\text{A}$  beam current it was possible to hold the potential within 5 keV of 2.00 MeV, over 48 hours, resulting in errors of  $\pm 0.25$  per cent in the normalised amplitudes. The corresponding error in phase was less than 0.001 radians.

It was observed that the lithium target yield declined by about 50 per cent during the first 48 hours of use, thereafter remaining steady. A comparison of the d.c. components of experiments with new and old targets revealed no systematic changes from this cause.

The palladium leaks used to supply gas to the ion source of the accelerator do allow a certain amount of seepage when normally switched off, the amount of leakage varying slowly with time. This resulted in contamination of the proton beam with deuterons and hence a variable amount of high neutron energy contamination (up to  $\sim 17$  MeV) from the  $\text{Li}^7(\text{d},\text{n})\text{Be}^8$  reaction. This gives rise to two possible sources of error.

(1) Systematic changes in the sub-cadmium neutron wave from experiment to experiment because of the changes in source condition.

(2) Changes in the normalisation within an experiment because of the different sensitivity of the monitor and movable detectors to the epi-cadmium component of the source.

An estimate of these effects can be made in the following way:

Let  $E$  be the count rate of the detector in the BeO when it is closest to the source and the cadmium shutter is interposed between the source and the stack.

$T$  be the count rate as above when the shutter is removed.

Then  $S=T-E$  is the count rate from the detector corresponding to the sub-cadmium component of the source.

The subscripts  $p$  and  $d$  will denote a neutron source due to the proton and deuteron reactions respectively. The cadmium ratio  $R$  is defined as:

$$R = (T_p + T_d) / (E_p + E_d)$$

The ratio  $T/E$  has been measured to be 1.20 for neutrons from the  ${}^9\text{Be}(d,n){}^{10}\text{B}$  reaction in experiments having a closely similar experimental configuration (Whittlestone 1968) and it is assumed that this ratio will not be too different from the ratio  $R_d = T_d/E_p$  for neutrons from the  ${}^7\text{Li}(d,n){}^8\text{Be}$  reactions. Values of  $R$  found during the experiments varied from 5.44 to 5.18 at the point closest to the source. Assuming that the largest cadmium ratio corresponded to zero deuterium contamination, that is taking  $R_p$  to be 5.44, then the fraction of the sub-cadmium count rate  $S_d/S_p$  that can be attributed to the fast neutron source for the experiment with most deuterium contamination ( $R = 5.18$ ) is 0.0028 (see Appendix A).

An independent check of this ratio  $S_d/S_p$  was obtained by measuring the count rate with the shutter removed when the proton energy was just below the  ${}^7\text{Li}(p,n){}^7\text{Be}$  threshold, which should give  $T_d$ , and the corresponding count rate at a proton energy of 2.0 MeV which should give  $T_d + T_p$ . Assuming the values  $R_p$  and  $R_d$  quoted above then two such measurements yielded cadmium ratio values  $R$  in the range found experimentally and  $S_d/S_p$  values of 0.00011 and 0.0015. This implies that the percentage

contribution of fast neutrons from  $\text{Li}^7(\text{d},\text{n})\text{Be}^8$  reaction to the sub-cadmium count rate was less than about 0.28 per cent. Although the measured wave is not a discrete mode it clearly consists of modes with a predominantly thermal distribution of energies and since the sub-cadmium neutrons from both reactions are essentially thermal, any systematic errors arising from the higher energy contamination of the source should be second order and are considered negligible.

Because of the partial cadmium cladding of the monitor detector the ratio of the count rate due to the high neutron energy contamination of the source to the count rate due to the low energy neutrons,  $M_d/M_p$ , will lie somewhere between  $T_d/T_p$  and  $E_d/E_p$ . For the experiment with the highest deuterium contamination ( $R = 5.18$ )  $T_d/T_p$  was 0.014 and  $E_d/E_p$  was 0.061 which implies that the monitor count rate could change by up to 6 per cent depending on the deuterium contamination in the beam. Long term errors in reproducibility of a few per cent have been attributed to this effect. It was possible to eliminate these changes in amplitude normalisation by a process of 're-normalising' the wave amplitudes. The time averaged amplitude at each position was taken to be the mean of the measurements of the time averaged amplitudes from five experiments. The wave amplitudes were then multiplied by the ratio of the mean time averaged amplitude to the time averaged amplitude associated with the given measurement. This technique resulted in reproducibility of wave amplitudes in the range 0.5 per cent to 1.0 per cent at positions close to the source.

The errors in the wave amplitudes calculated by the fitting program varied from 0.1 per cent at 515.7 Hz for positions close to the source to 25 per cent at 1718.9 Hz for positions distant from the source, and the errors in phases from 0.003 radians to 0.15 radians. In view of the discussion in the previous paragraph, the errors calculated for points close to the source were unduly optimistic. A minimum error in the phases and re-normalised amplitudes was established for each experiment on the basis of the reproducibility of measurements from points within 17 cm of the source. Where the calculated error was less than this minimum error, the error assigned to a given amplitude or phase was increased to the minimum error.

The final estimates of the errors in amplitude ranged from 0.5 per cent to 3 per cent 7.6 cm from the source and from 1.3 per cent to 25 per cent 47.6 cm from the source. The corresponding ranges of error in phases were 0.007 to 0.02 radians and 0.015 to 0.15 radians.

#### 4. RESULTS AND DISCUSSION

The experimental amplitudes and phases are given in Table 1 and figures 1 and 2. They have been normalised to the standard reference density of  $2.96 \text{ cm}^{-3}$  by applying the appropriate density corrections to the frequencies ( $\omega = \omega' \times \rho/\rho'$ ) and distances ( $z = z' \times \rho'/\rho$ ), where the dash indicates the experimentally measured quantity. Experiment B at 982.3 Hz was carried out using three inches of polythene moderator, while all other experiments were carried out using two inches of polythene.

To determine the frequencies for which a discrete mode of propagation is compatible with the experimental results in the sense that  $\alpha$  and  $\xi$  do not change with distance, 'local' attenuation and phase shift parameters (figures 3 and 4) have been obtained from a least squares fit of the data over approximately 10 cm intervals to the form

$$R(z)e^{i\phi(z)} = Ae^{i\theta}(e^{-\rho z} - e^{-\rho(2L-z)}) \quad \dots(1)$$

where  $z$  = distance from source  
 $R(z)$  = amplitude of the wave  
 $\phi(z)$  = phase shift of the wave  
 $L$  = extrapolated length of the BeO assembly  
 $\rho = \alpha - i\xi$

where  $\alpha$  = attenuation parameter  
 $\xi$  = phase shift parameter  
 $A$  and  $\theta$  are constants which depend on the amplitude and phase of the wave at  $z=0$ .

It should be noted that the quantities  $\alpha(z)$  and  $\xi(z)$  shown in figures 3 and 4 are the  $\alpha$  and  $\xi$  parameters derived from the intervals  $z$  to  $z + \Delta z$  where  $\Delta z \lesssim 10 \text{ cm}$  and hence are not all statistically independent. This requires some care in the interpretation of the figures.

It is apparent from figures 3 and 4 that  $\alpha$  and  $\xi$  vary continuously with distance from the source at frequencies of 982.3 Hz or greater, while both parameters vary only slightly at 515.3 Hz. As an additional criterion for compatibility with a discrete mode of decay, the ability of the  $A(z)$  and  $\phi(z)$  data to conform with the expression (1) over the distance range 9 to 47 cm from the source was used. Analysis of the fits proved that the results of the 515.7 Hz experiment are consistent with a discrete mode of propagation ( $P(\chi^2) = 0.39$ ) in agreement with previous findings (Ritchie and Whittlestone 1971), but that the results of the 736.6 Hz experiment are not ( $P(\chi^2) = 0.012$ ).

The extra inch of polythene used in experiment B at 982.3 Hz had no measurable effect on the time averaged component of the neutron wave. Using the method described in appendix B, the spatial variation of the amplitude of the time averaged component measured using three inches of polythene moderator was found to be compatible ( $P(\chi^2) = 0.45$ ) with the mean of the other two experiments where the errors on the amplitudes were  $\sim 0.5$  per cent in all cases. However, the amplitudes and phases of the fundamental wave measured using the thicker polythene (experiment B) were significantly different from the properties measured using the thinner polythene (experiments A and C). This can be noted in figures 3 and 4 where the result of experiment B showed less variation with distance than those of A or C. Again using the method of appendix B it can be shown that experiment B is not compatible ( $P(\chi^2) = 10^{-5}$ ) with either A or C where A and C are consistent with each other ( $P(\chi^2) = 0.14$ ) as is to be expected.

The deviation of the wave parameters measured at 982.3 Hz from a discrete mode of propagation can be quantified in the following way. Both  $\alpha(z)$  and  $\xi(z)$  can clearly be fitted with the form

$$\begin{aligned}\alpha(z) &= az^2 + bz + c, \\ \xi(z) &\end{aligned}$$

It is also clear that the first order term  $b$  will be very small and that the second order term, which will be close to the curvature of the curve, will provide an index of how much  $\alpha(z)$  or  $\xi(z)$  deviate from a constant. The second order terms along with the cadmium ratios for the experiments A, B and C are given in Table 2. It is evident that the wave parameters from the experiment with the thicker polythene vary less with distance than those measured using the thinner polythene. This result is somewhat unexpected as the thicker polythene leads to a source with a significantly higher cadmium ratio (11.2 compared to 5.3) and hence, one would expect a higher sub-Bragg component and hence a more pronounced deviation from an apparently discrete mode of propagation.

Figure 5 shows the spatial variation of the local attenuation and phase shift parameters at a frequency  $\sim 500$  Hz compared with those predicted by Wood(1971) for a BeO assembly of similar buckling. The experimental  $\alpha(z)$  and  $\xi(z)$  have been derived from non-overlapping spatial intervals and hence are statistically independent parameters. The feature of interest in this figure is the qualitative agreement in the

spatial variation of those parameters, which should be little affected by the lower frequency, 506.1 Hz compared to 515.7 Hz, and lower buckling,  $0.00483 \text{ cm}^{-2}$  compared to  $0.00513 \text{ cm}^{-2}$ , used in the theoretical calculations compared to those used in the experiment. It can be seen that theory predicts a variation with distance not seen in the experimental results. This is particularly true of the parameter  $\alpha(z)$  which theory predicts varies by a total of  $\sim 11$  per cent over the distance range 9 - 35 cm whereas experiment shows it to be constant within the errors of  $\lesssim 1$  per cent. The increasing  $\alpha(z)$  predicted by Wood would also indicate an interference minimum at  $z > 40$  cm from the source of which there is no sign in the experimental results. It should be noted, however, that Wood's calculations assumed a source with a Maxwellian distribution of energies. The experimental results of Utsuro et al. (1968) and indeed the present experiment at 983.2 Hz indicate the sensitivity of measured wave parameters to the source conditions. Hence it would seem most likely that a major cause of the discrepancy between theory and experiment is the over simplified representation of the source conditions assumed in the theoretical calculations.

Figures 6 and 7 show the experimental amplitudes  $A(z)$  and phases  $\phi(z)$  at frequencies 515.7, 982.3 and 1473.3 Hz and theoretical predictions at these frequencies derived from the work of Wood and Lawrence (Private Communication 1971). Again there is poor agreement between the spatial variation of these quantities predicted by theory and that seen experimentally except in the case of  $\phi(z)$  at 515.7 Hz. The theoretical amplitude  $A(z)$  at 515.7 Hz shows a curvature not seen in the experimental results while the theoretical  $A(z)$  and  $\phi(z)$  at 982.3 and 1473.3 Hz show interference effects not present in the experimental results. Indeed the theoretical  $\phi(z)$  show an interference effect typical of just two wave interference. Wood and Lawrence give no details of the counter size used in their calculations. Simple calculations indicate that the counter length in the  $z$  direction will influence both the position and amplitude of interference effects particularly at high frequencies where the parameter  $\xi(z)$  is quite large, an effect noted in the theoretical calculations of Nishina and Akcasu (1970). Moreover, Wood and Lawrence assume once again a source with a Maxwellian energy distribution which almost certainly is inadequate for the present system. It is worth emphasising that unambiguous comparisons between theory and experiment in such experiments require that as much as possible of the source energy distribution, source geometry, assembly geometry and detector size and energy response be taken into account.

Figure 8 shows a plot of the dispersion relations for a neutron wave in BeO derived from both the present and previous experiments (Ritchie and Whittlestone 1971). The solid curve indicates that region of the  $(\alpha, \xi)$  plane where the attenuation and phase shift parameters of the wave are not significantly different from those of a discrete mode in the sense that any changes of these parameters with distance from the source are less than the experimental errors. The shaded region of the  $(\alpha, \xi)$  plane indicates that the values of  $\alpha$  and  $\xi$  found for the wave depend on both the frequency  $\omega$  and position  $z$ . The transition region is about 500 Hz. At or below 516 Hz the wave can be described by a discrete mode while at 736 Hz or above it can not be described by a discrete mode. The close similarity between the import of this figure and the figure for the effective  $\lambda(B^2)$  relationship in BeO (Rainbow and Ritchie 1968) should be noted.

## 5. CONCLUSIONS

The present experiments confirm the previous observations that below a frequency of  $\sim 520$  Hz in BeO a mode of wave propagation exists which has all the appearances of a discrete mode. This is at variance with the theoretical predictions of Wood which show that at frequencies well below this the attenuation and phase shift parameters should change significantly with distance. Wood assumed a Maxwellian distribution of energies in this source which is almost certainly not true for the source used in the present investigation. It is felt that this is the major reason for the present discrepancy between theory and experiment. It is suggested that further calculations are required both to investigate the sensitivity of the parameters  $\alpha(z)$  and  $\xi(z)$  to the source conditions and to produce parameters that correspond more closely to the system described in the present set of experiments.

At frequencies greater than  $\sim 520$  Hz the wave properties are no longer consistent with those of a discrete mode of propagation. However, there is no sign of the interference effects predicted by Wood and Lawrence. Again since the amplitude and position of such interference effects will depend critically on the initial source conditions and the size, orientation and energy response of the detectors it is suggested that again further calculations are required taking more detailed account of these parameters.

6. REFERENCES

- Duderstadt, D.D. (1968) - Nucl. Sci. Eng. 33, 119.
- Fraser, H.J., Ritchie, A.I.M. and Whittlestone, S. (1968) - Rev. Scient. Instrum. 39, 240.
- Nishina and Akcasu (1970) - Nucl. Sci. Eng. 39, 170.
- Rainbow, M.T. and Ritchie, A.I.M. (1968) - J. Nucl. Energy, 22, 735.
- Ritchie, A.I.M. and Whittlestone, S. (1971) - J. Nucl. Energy. In Press.
- Ritchie, A.I.M. (1968) - J. Nucl. Energy, 22, 371.
- Takahashi, A. and Sumita, K. (1968a) - J. Nucl. Sci. Technol. 5, 7.
- Takahashi, A. and Sumita, K. (1968b) - J. Nucl. Sci. Technol. 5, 132.
- Utsuro, M., Inoue, K. and Shibata, T. (1968) - J. Nucl. Sci. Technol. 5, 298.
- Utsuro, M. and Shibata, T. (1967) - J. Nucl. Sci. Technol. 4, 205.
- Whittlestone, S. (1968) - M.Sc. Thesis, University of New South Wales, Australia.
- Williams, M.M.R. (1968) - Neutron Thermalisation and Reactor Spectra Vol. 1, p. 27, IAEA Vienna.
- Wood, J. (1969) - J. Nucl. Energy, 23, 211.
- Wood, J. (1971) - J. Nucl. Energy, 25, 132.



## APPENDIX A

### DERIVATION OF $S_d/S_p$ , $E_d/E_p$ AND $T_d/T_p$ FROM CADMIUM RATIOS

The measured parameters are:

1.  $R = (T_p + T_d) / (E_p + E_d)$  cadmium ratio for the given experiment
2.  $R_p = T_p / E_p$  cadmium ratio with proton beam only
3.  $R_d = T_d / E_d$  cadmium ratio with deuteron beam only
4.  $S_d = T_d - E_d$
5.  $S_p = T_p - E_p$

Equations 1 - 5 may be solved to yield:

6.  $T_d/T_p = (1 - R/R_p) / (R/R_d - 1)$
7.  $E_d/E_p = (R - R_p) / (R_d - R)$
8.  $S_d/S_p = \left( \frac{R_p - R}{R_p - 1} \right) \left( \frac{R_d - 1}{R - R_d} \right)$

1

2

3

## APPENDIX B

Direct comparison of two wave experiments is not possible because the amplitude and phase at the origin depend on the position of the monitor counter in the polythene and the amount of polythene used. To determine the probability that two experiments are compatible, the amplitudes of one experiment are multiplied by a factor  $f$ , while a zero position phase shift  $\theta$  is added to the phases.  $f$  and  $\theta$  are chosen to minimise the sum:

$$\chi^2 = \sum_{i=1}^N \left[ \frac{(A_i - f B_i)^2}{(\delta A_i)^2 + (f \delta B_i)^2} + \frac{(\xi_i - \mu_i - \theta)^2}{(\delta \xi_i)^2 + \delta \mu_i^2} \right]$$

where the summation is over all the  $N$  space points

$A_i$  and  $\xi_i$  are the amplitudes and phases of one experiment

$B_i$  and  $\mu_i$  are the amplitudes and phases of the other experiment

$\chi^2$  has its usual significance.

$P(\chi^2)$ , the integral of the  $\chi^2$  distribution for  $2N-2$  degrees of freedom from  $\chi^2$  to infinity, gives the probability of obtaining the observed or a larger value of  $\chi^2$ .



TABLE I

Compilation of amplitudes and phases from neutron wave experiments in BeO, at frequencies 515.7, 736.6, 982.3, 1473.3 and 1719.0 Hz, normalised to a density of  $2.96 \text{ g cm}^{-3}$ .

## FREQUENCY 515.7 HZ

POSITION CM	AMPLITUDE	ERROR	PHASE RADIAN	ERRCR RADIAN
7.35	10.72000	0.10000	1.282	0.020
7.35	10.59000	0.10000	1.235	0.020
9.77	7.69400	0.08000	1.431	0.020
12.20	5.72720	0.05700	1.703	0.020
12.20	5.63950	0.05700	1.646	0.020
14.62	4.17380	0.04300	1.879	0.020
17.05	3.02830	0.02800	2.120	0.020
17.05	3.00830	0.02900	2.101	0.020
19.47	2.19400	0.02100	2.321	0.020
21.89	1.60770	0.01400	2.569	0.020
21.89	1.58850	0.01600	2.549	0.020
24.32	1.16510	0.01200	2.776	0.020
26.74	0.85096	0.00660	3.013	0.020
26.74	0.84943	0.00620	2.996	0.020
29.17	0.62643	0.00580	3.230	0.020
31.59	0.46320	0.00560	3.481	0.020
34.01	0.34039	0.00530	3.682	0.020
36.44	0.26065	0.00480	3.959	0.020
36.44	0.24569	0.00500	3.882	0.020
38.86	0.18691	0.00410	4.128	0.020
41.29	0.13903	0.00310	4.351	0.020
41.29	0.13630	0.00310	4.330	0.020
43.71	0.10155	0.00220	4.522	0.020
46.13	0.07449	0.00180	4.682	0.020
46.13	0.07168	0.00170	4.673	0.020

## FREQUENCY 736.6 HZ

POSITION CM	AMPLITUDE	ERROR	PHASE RADIAN	ERRCR RADIAN
7.35	10.41200	0.08700	1.554	0.007
14.62	3.51690	0.03500	2.289	0.007
17.05	2.42100	0.02300	2.568	0.007
17.05	2.43490	0.02300	2.557	0.007
19.47	1.68660	0.01700	2.824	0.006
21.89	1.14960	0.01200	3.110	0.006
24.32	0.79789	0.00820	3.386	0.006
26.74	0.54869	0.00600	3.668	0.007
26.74	0.55246	0.00600	3.661	0.007
29.17	0.38931	0.00400	3.940	0.010
31.59	0.26821	0.00250	4.215	0.010
34.01	0.18743	0.00180	4.499	0.012
36.44	0.13710	0.00140	4.777	0.012
36.44	0.13612	0.00140	4.782	0.012
41.29	0.06734	0.00090	5.328	0.013
41.29	0.06880	0.00090	5.315	0.013
43.71	0.04919	0.00062	5.556	0.015
46.13	0.03484	0.00062	5.773	0.015
46.13	0.03531	0.00062	5.773	0.018



TABLE I Contd.

FREQUENCY 982.3 HZ A

POSITION CM	AMPLITUDE	ERROR	PHASE RADIAN	ERRCR RADIAN
7.35	8.85280	0.04300	1.841	0.007
9.77	5.85600	0.03100	2.134	0.007
12.20	3.86360	0.03200	2.426	0.007
12.20	3.85580	0.03200	2.426	0.010
14.62	2.52230	0.01600	2.728	0.010
17.05	1.63030	0.01100	3.012	0.010
17.05	1.65450	0.01100	3.036	0.010
19.47	1.08140	0.00770	3.356	0.010
21.89	0.70677	0.00570	3.671	0.010
21.89	0.70024	0.00400	3.685	0.010
24.32	0.45726	0.00280	4.014	0.010
26.74	0.30510	0.00200	4.336	0.010
26.74	0.30363	0.00180	4.355	0.010
31.59	0.13524	0.00090	5.026	0.010
31.59	0.13604	0.00102	5.012	0.010
34.01	0.09221	0.00077	5.348	0.010
36.44	0.06390	0.00057	5.676	0.010
36.44	0.06373	0.00057	5.695	0.010
41.29	0.02973	0.00030	6.317	0.010
41.29	0.03044	0.00029	6.314	0.010
43.71	0.02119	0.00023	6.615	0.010
46.13	0.01529	0.00019	6.897	0.015

FREQUENCY 982.3 HZ B

POSITION CM	AMPLITUDE	ERROR	PHASE RADIAN	ERRCR RADIAN
7.35	10.40000	0.05000	2.114	0.014
7.35	10.20900	0.07000	2.104	0.019
9.77	6.77500	0.04700	2.408	0.013
12.20	4.48130	0.02800	2.715	0.010
12.20	4.47370	0.03000	2.718	0.010
14.62	2.95000	0.01900	3.035	0.010
17.05	1.95220	0.01300	3.356	0.010
19.47	1.27090	0.00950	3.677	0.011
21.89	0.84642	0.00650	4.012	0.012
21.89	0.85100	0.00650	4.008	0.013
24.32	0.56482	0.00470	4.347	0.023
26.74	0.38457	0.00330	4.667	0.019
29.17	0.24700	0.00230	5.003	0.020
31.59	0.16570	0.00160	5.341	0.015
31.59	0.16730	0.00170	5.335	0.017
34.01	0.10989	0.00130	5.667	0.015
36.44	0.07659	0.00090	6.002	0.012
36.44	0.07780	0.00090	6.001	0.012
38.86	0.04811	0.00070	6.382	0.018
41.29	0.03756	0.00055	6.635	0.020
43.71	0.02496	0.00037	7.084	0.025
46.13	0.01895	0.00030	7.237	0.030





TABLE I Contd.

FREQUENCY 982.3 HZ C

POSITION CM	AMPLITUDE	ERROR	PHASE RADIAN	ERRCR RADIAN
7.86	5.98600	0.06500	1.868	0.008
10.29	4.05080	0.06000	2.152	0.008
12.71	2.69400	0.05500	2.449	0.008
15.14	1.72610	0.03200	2.741	0.008
17.56	1.12200	0.02400	3.020	0.008
19.98	0.71908	0.01700	3.356	0.008
22.41	0.47855	0.01300	3.687	0.010
24.83	0.31235	0.00700	4.013	0.010
27.26	0.20806	0.00380	4.341	0.012
29.68	0.13450	0.00250	4.686	0.012
32.10	0.09096	0.00190	5.030	0.014
34.53	0.06189	0.00135	5.357	0.016
36.95	0.04161	0.00095	5.669	0.020
39.38	0.02772	0.00070	5.981	0.020
41.80	0.01941	0.00050	6.268	0.026
44.22	0.01344	0.00035	6.615	0.026
46.65	0.00978	0.00030	6.887	0.030

FREQUENCY 1473.3 HZ

POSITION CM	AMPLITUDE	ERROR	PHASE RADIAN	ERRCR RADIAN
7.35	5.23160	0.03823	2.320	0.008
7.35	5.23570	0.03163	2.330	0.007
7.35	5.26000	0.02845	2.319	0.006
9.77	3.16590	0.01805	2.659	0.014
12.20	1.89680	0.01659	3.017	0.007
12.20	1.88440	0.01498	3.008	0.006
12.20	1.89200	0.01305	3.020	0.005
14.62	1.10620	0.00928	3.391	0.006
17.05	0.63714	0.00691	3.774	0.010
17.05	0.65449	0.00779	3.779	0.011
17.05	0.65015	0.00661	3.779	0.010
19.47	0.38726	0.00478	4.193	0.015
21.89	0.22421	0.00384	4.603	0.020
21.89	0.22510	0.00391	4.626	0.020
21.89	0.22300	0.00358	4.624	0.020
24.32	0.13459	0.00280	5.114	0.020
26.74	0.07975	0.00219	5.547	0.020
26.74	0.08420	0.00219	5.523	0.020
26.74	0.08290	0.00214	5.519	0.025
29.17	0.05247	0.00174	6.021	0.025
31.59	0.03524	0.00139	6.388	0.025
34.01	0.02304	0.00097	6.811	0.025
36.44	0.01636	0.00096	7.224	0.025
38.86	0.01062	0.00073	7.576	0.025
41.29	0.00752	0.00055	7.996	0.025
41.29	0.00730	0.00052	8.022	0.025
43.71	0.00555	0.00042	8.458	0.030
46.13	0.00344	0.00031	8.783	0.030



TABLE I Contd.

FREQUENCY 1719.0 HZ

POSITION CM	AMPLITUDE	ERROR	PHASE RADIAN	ERROR RADIAN
7.36	2.82700	0.07600	2.033	0.010
7.36	2.82600	0.07000	2.041	0.010
7.84	2.70050	0.06070	2.095	0.015
8.81	2.12400	0.06000	2.214	0.015
8.81	2.14000	0.06000	2.211	0.015
8.81	2.15200	0.05650	2.219	0.015
8.81	2.04030	0.08700	2.247	0.015
12.21	0.94410	0.03100	2.723	0.015
12.69	0.93990	0.03100	2.727	0.015
13.66	0.69950	0.02260	2.914	0.015
14.15	0.64170	0.02800	2.965	0.020
14.63	0.53370	0.01900	3.097	0.020
17.06	0.29530	0.01190	3.500	0.020
17.54	0.26770	0.00950	3.580	0.020
18.99	0.19920	0.00860	3.820	0.020
19.48	0.15490	0.00770	3.938	0.020
19.48	0.15950	0.00720	3.924	0.020
19.96	0.14860	0.00750	4.014	0.020
21.90	0.07872	0.00390	4.522	0.020
22.39	0.07240	0.00430	4.554	0.020
24.33	0.04910	0.00300	4.948	0.020
24.81	0.04710	0.00320	5.017	0.030
26.75	0.02877	0.00210	5.518	0.030
27.24	0.02490	0.00190	5.616	0.030
29.18	0.01994	0.00150	6.134	0.040
29.66	0.01880	0.00160	6.199	0.040
32.08	0.01029	0.00110	6.771	0.050
34.51	0.00776	0.00103	7.182	0.050
36.93	0.00485	0.00082	7.628	0.070
38.19	0.00321	0.00061	7.688	0.070
41.78	0.00187	0.00091	8.644	0.100
43.04	0.00184	0.00050	8.842	0.100
46.63	0.00120	0.00030	8.829	0.150



TABLE 2

EFFECT OF SOURCE CONDITIONS ON 982.3 Hz NEUTRON WAVE

Experiment	Cadmium Ratio	Second Derivatives	
		$\alpha''(z) \text{ cm}^{-3} \times 10^6$	$\xi''(z) \text{ cm}^{-3} \times 10^6$
A	5.24	61.6 $\pm$ 4.8	128.6 $\pm$ 5.6
B	11.45	45.6 $\pm$ 7.0	34.6 $\pm$ 8.4
C	5.18	63 $\pm$ 13	149 $\pm$ 10



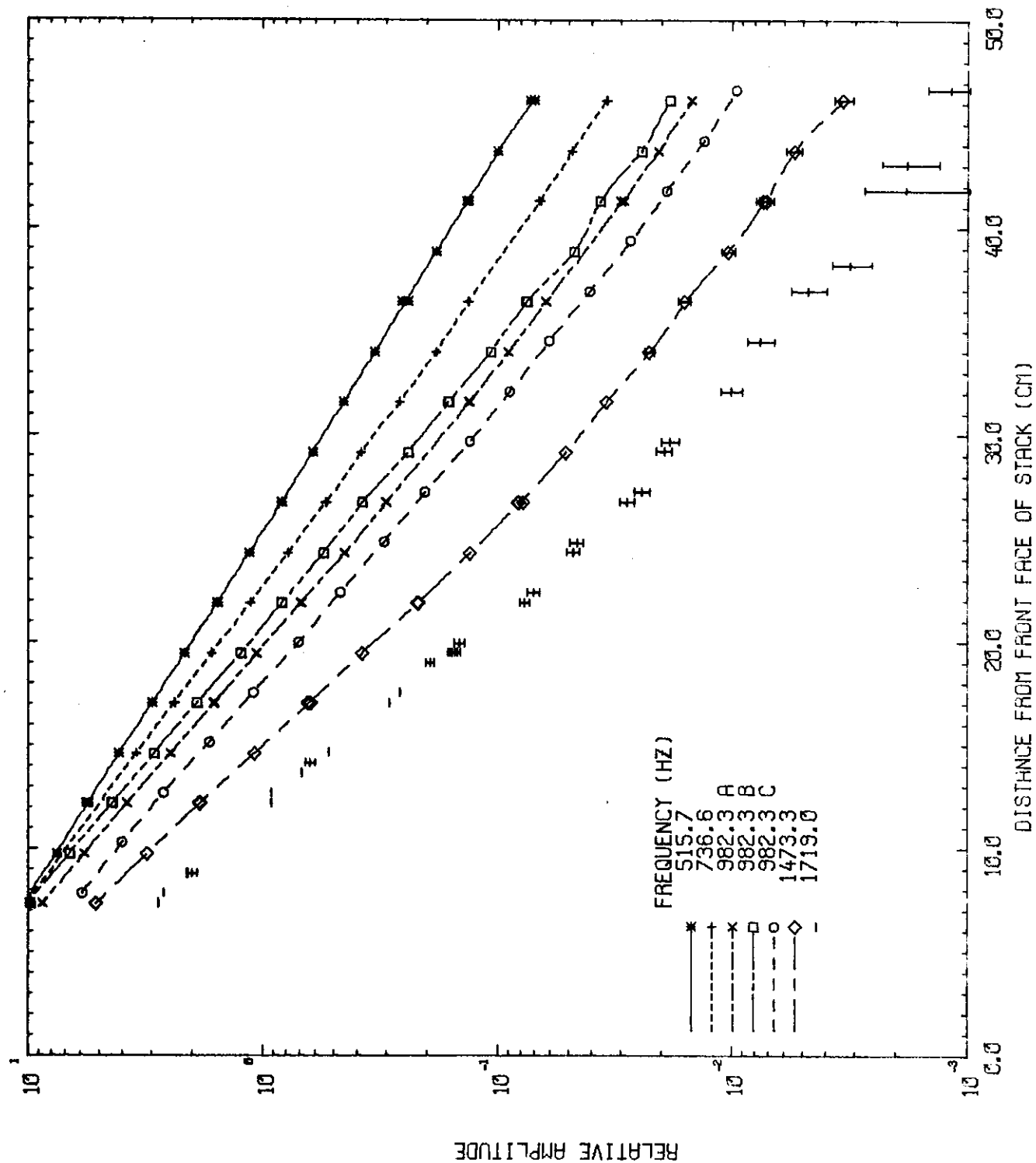


FIGURE 1. NEUTRON WAVE AMPLITUDES FOR BeO OF DENSITY 2.96 g cm<sup>-3</sup>





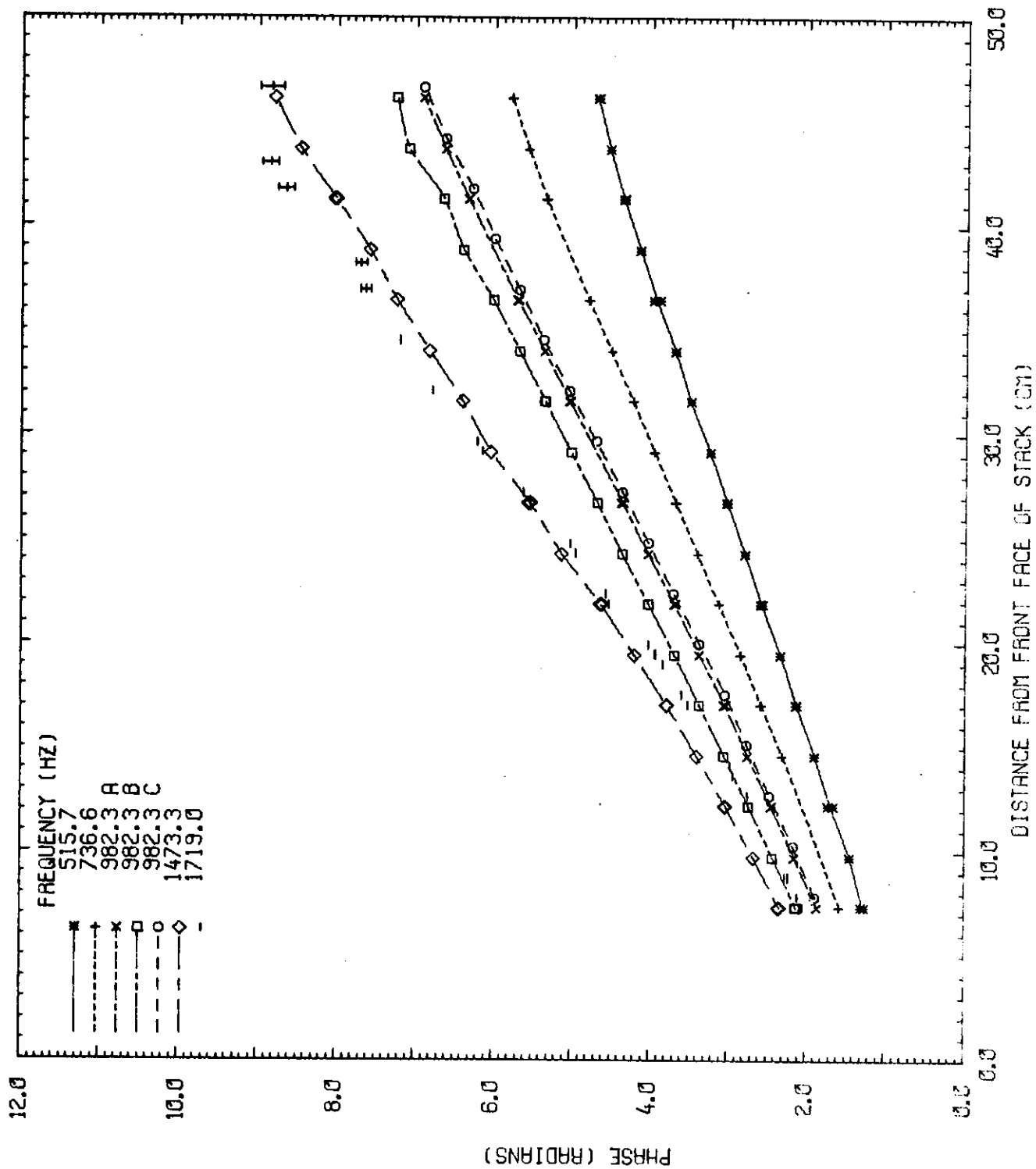


FIGURE 2. NEUTRON WAVE PHASES FOR BeO OF DENSITY 2.96g cm<sup>-3</sup>



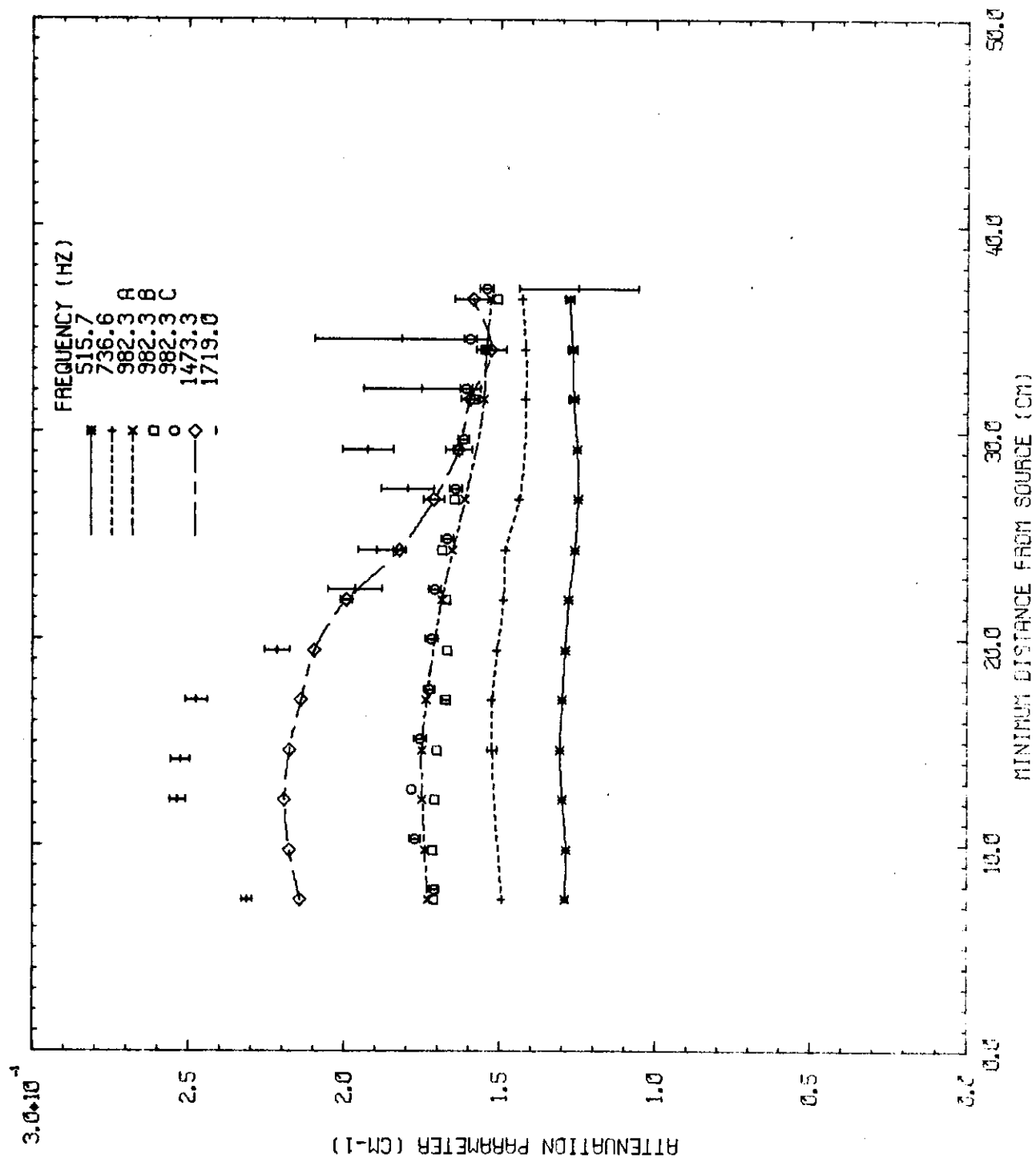


FIGURE 3. NEUTRON WAVE ATTENUATION PARAMETERS DERIVED FROM FITS TO DATA BETWEEN Z AND Z + 10 cm FROM THE SOURCE,  $Z \geq 7.35$  cm



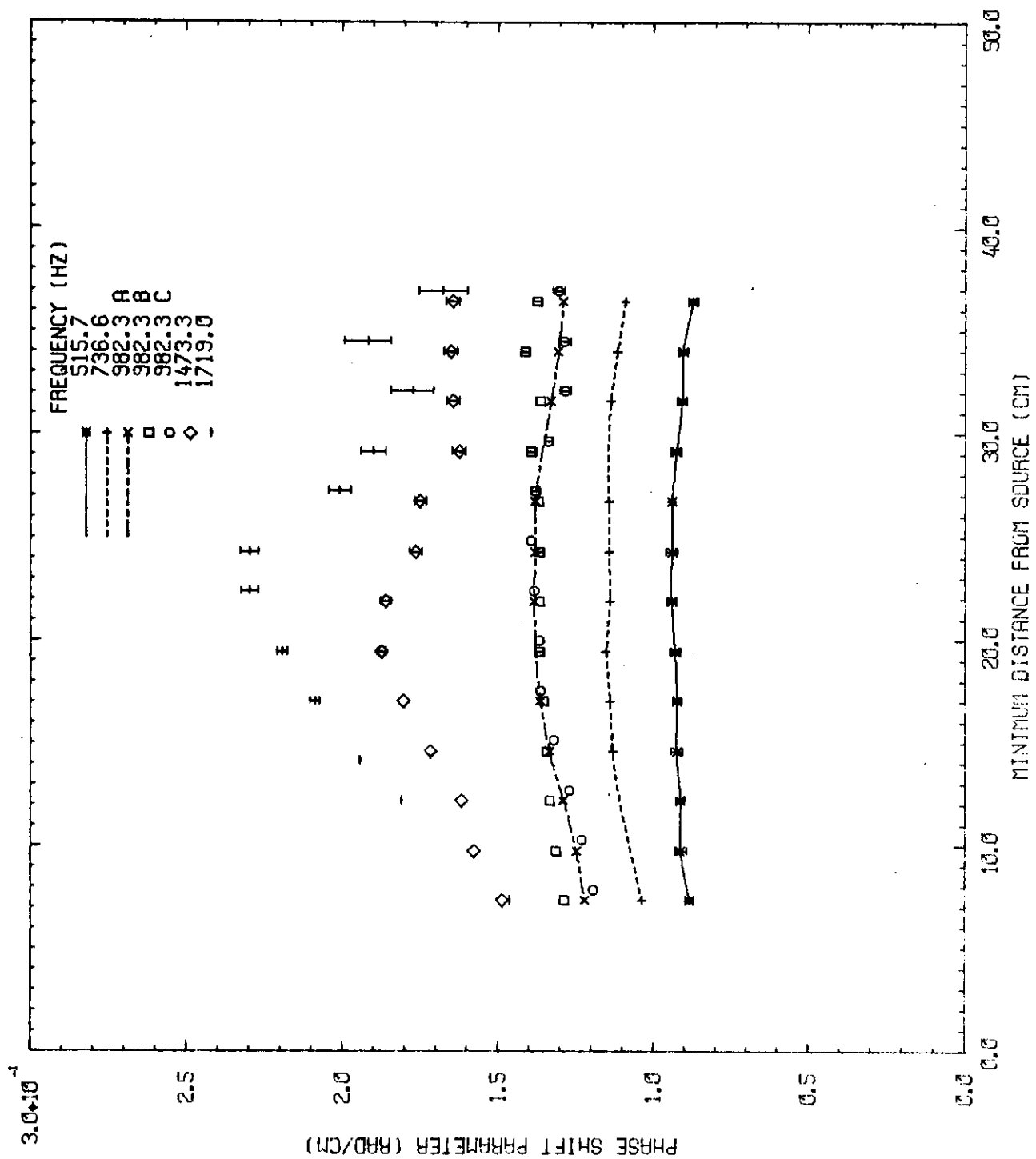
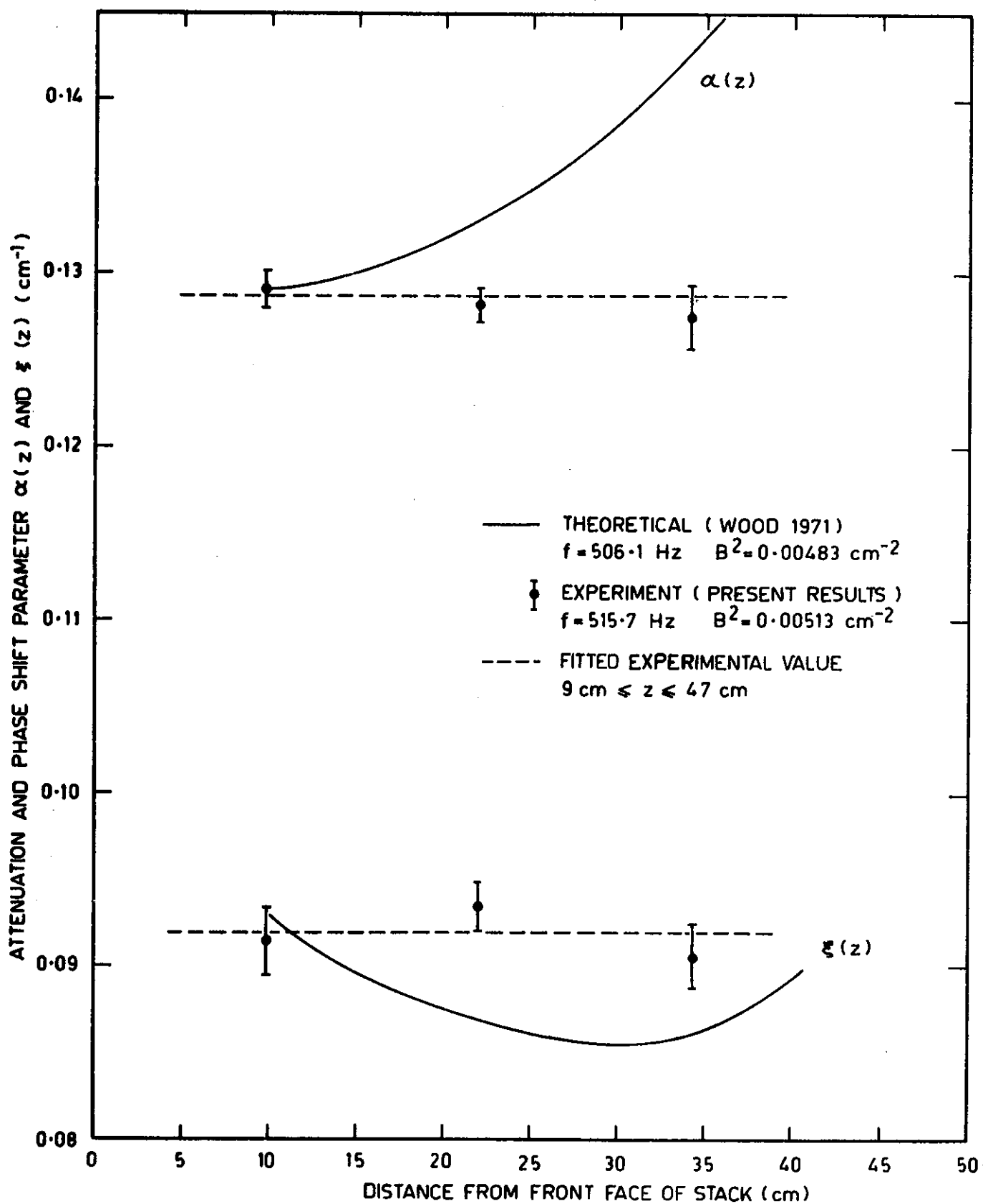


FIGURE 4. NEUTRON WAVE PHASE SHIFT PARAMETERS DERIVED FROM FITS TO DATA BETWEEN Z AND Z + 10 cm FROM THE SOURCE,  $Z \geq 7.35$  cm





**FIGURE 5. COMPARISON BETWEEN THEORETICAL AND EXPERIMENTAL  $\alpha(z)$  AND  $\xi(z)$**





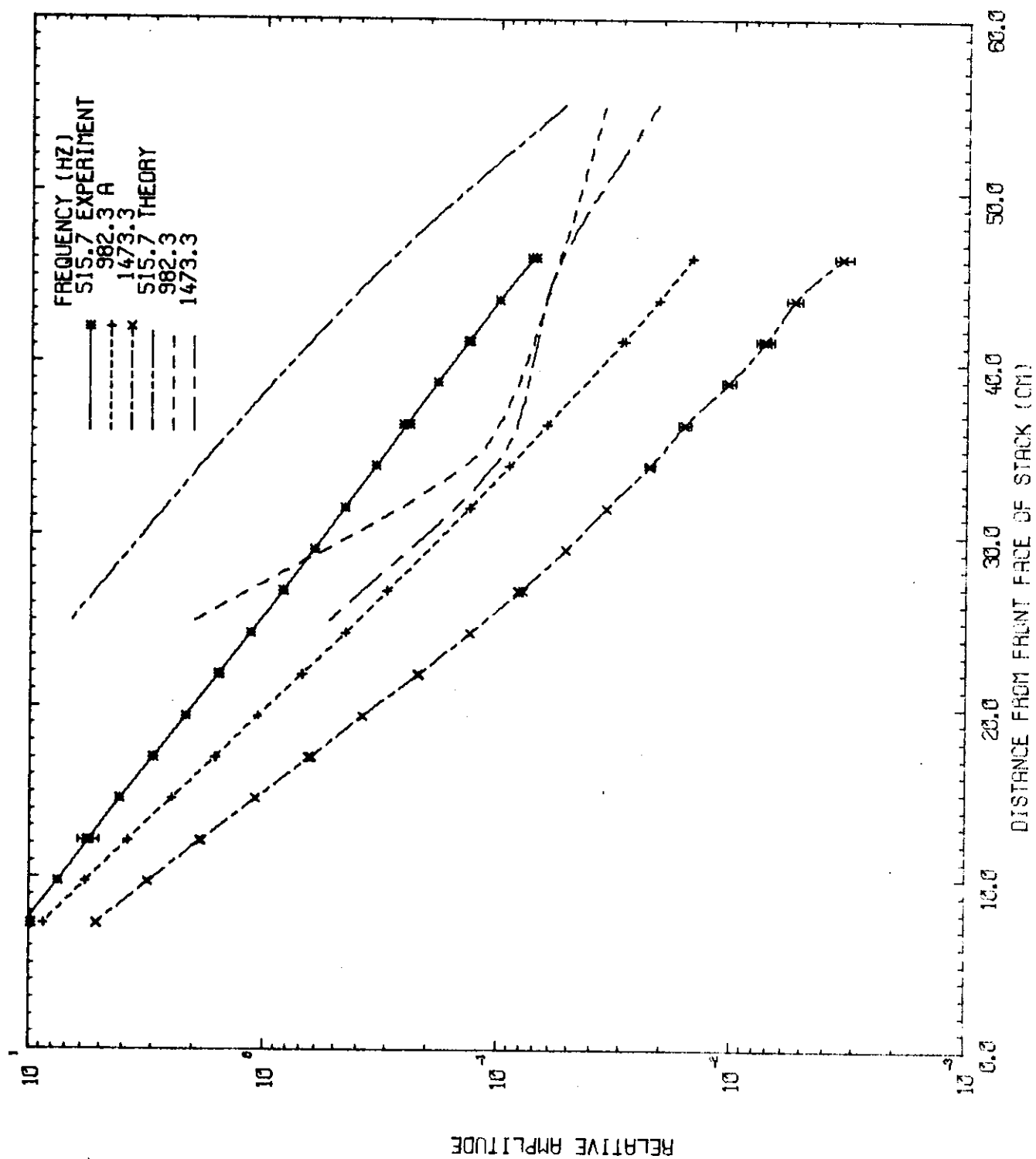


**FIGURE 6. COMPARISON OF EXPERIMENTAL AND THEORETICAL AMPLITUDES**



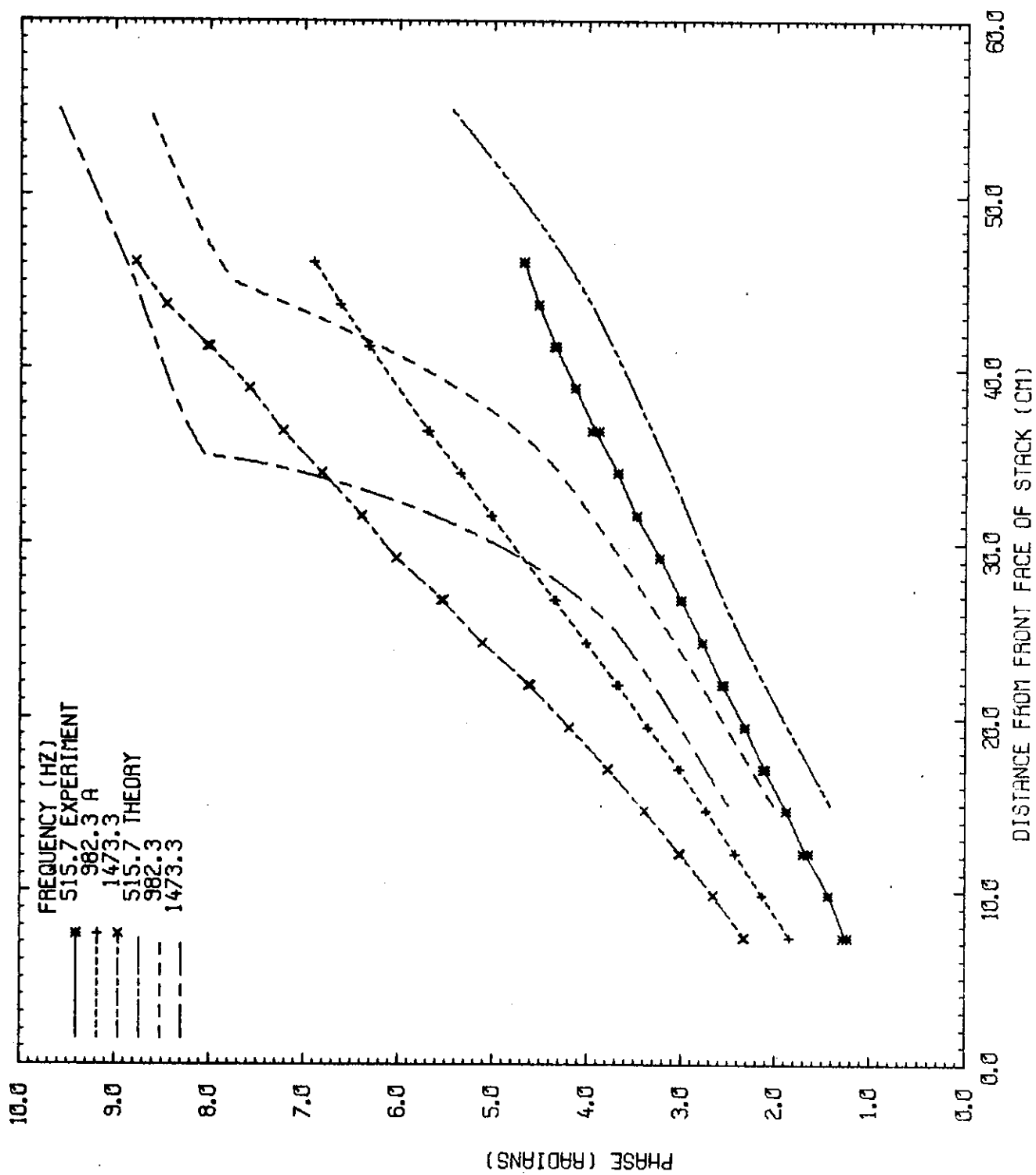


**FIGURE 7. COMPARISON OF EXPERIMENTAL AND THEORETICAL PHASES**



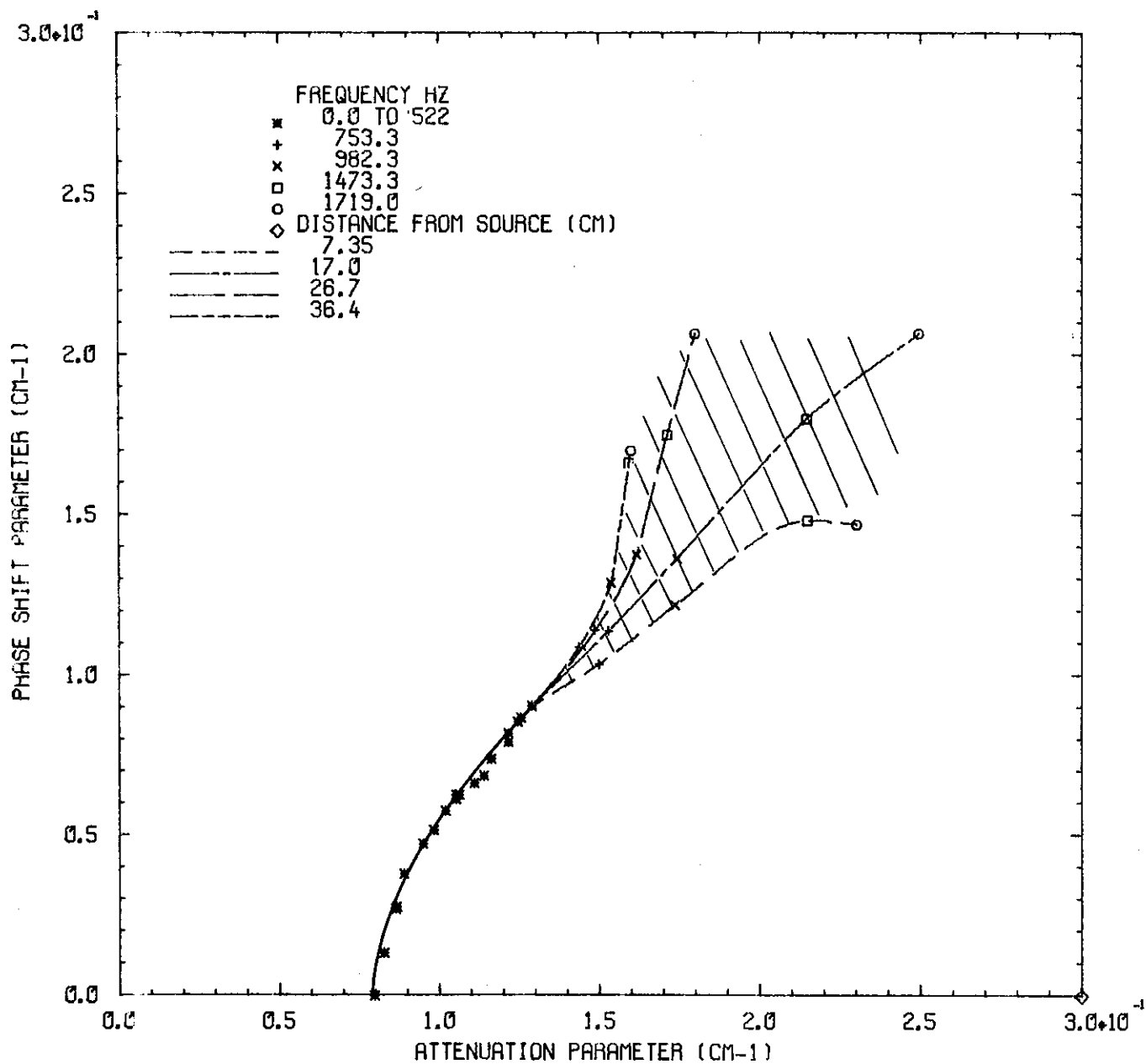


FIGURE 8. DISPERSION RELATIONS FOR NEUTRONS IN BeO FOR AN  
 ASSEMBLY WITH  $B^2 = 0.00513 \text{ cm}^{-2}$

